




The 16 September 2015 Illapel Earthquake and Tsunami: Post-Event Tsunami Inundation, Building and Infrastructure Damage Survey in Coquimbo, Chile

RYAN PAULIK,¹  JAMES H. WILLIAMS,² NICK HORSPOOL,³ PATRICIO A. CATALAN,^{4,5,6} RICHARD MOWLL,⁷
PABLO CORTÉS,⁴ and RICHARD WOODS³

Abstract—The 16 September 2015 M_w 8.3 Illapel Earthquake generated a tsunami that caused severe building and infrastructure damage in Coquimbo, Chile. Initial reports indicated numerous buildings, transport, energy, water and coastal protection structures sustained varying levels of damage in response to tsunami exposure. A digital ‘census style’ survey was carried out in Coquimbo to measure and record tsunami hazard characteristics and associated buildings and infrastructure network component damage. Flow depths measured from 655 watermarks ranged from 0.1 to 4.7 m, with a 1.47 m mean and 1.02 m standard deviation. Over 3000 damage samples were recorded for tsunami exposed buildings and infrastructure components. Damage levels for 545 buildings showed most sustained partial but repairable damage at tsunami flow depths up to 2 m. A further 2544 damage samples were collected for transport, energy, water infrastructure network components and coastal protection structures. We observed undamaged infrastructure components in high proportions and observed that complete component damage was often caused by secondary hazards (e.g. debris) or cascading impacts where seawall and stormwater culvert failures damaged co-located roads, pathways and utility poles. Future investigations of the hydrodynamic tsunami characteristics influencing infrastructure component fragility will support the analysis of physical damage to single components and cascading impacts across multiple infrastructure networks.

Keywords: Tsunami, inundation, buildings, infrastructure, post-event survey, Chile.

1. Introduction

On 16 September 2015, a large earthquake struck off the central Chile coast at 19:54 pm local time. The United States Geological Survey reported a subduction earthquake of moment magnitude (M_w) 8.3 had occurred about 48 km west of Illapel (Fig. 1a), with an epicentre at 31.573°S, 71.674°W and shallow depth of 22.4 km (USGS, 2015). The earthquake ruptured a \sim 240 km section of the Nazca–South American plate interface (Ye et al. 2016), generating a near-field tsunami for Chile. The Chilean Navy Hydrographic and Oceanographic Service (SHOA) issued a tsunami event warning eight minutes after the earthquake, followed three minutes later by the National Emergency Office (ONEMI) issuing a country-wide order to evacuate around one million residents from low-lying coastal land. In the following days, ONEMI reported 15 deaths along with 2442 destroyed and 2712 damaged houses from La Serena to Concón, Valparaíso (ONEMI 2015).

The 2015 Illapel Tsunami (Fig. 1a) was Chile’s third damaging near-field tsunami event since 2010. The event motivated several post-event field surveys, with teams measuring and recording tsunami hazard characteristics and damage along a 700 km stretch of coastline from Chañaral to Concón (Aranguiz et al. 2016; Tomita et al. 2016). Horizontal inundation and run-up measurements were mostly taken between La Serena and Los Vilos (Aranguiz et al. 2016) with

Supplementary Information The online version contains supplementary material available at <https://doi.org/10.1007/s00024-021-02734-x>.

¹ National Institute of Water and Atmospheric Research (NIWA), 301 Evans Bay, Greta Point, Wellington 6021, New Zealand. E-mail: ryan.paulik@niwa.co.nz

² School of Earth and Environment, University of Canterbury, 20 Kirkwood Ave, Christchurch 8041, New Zealand.

³ GNS Science, 1 Fairway Drive, Avalon, Lower Hutt 5010, New Zealand.

⁴ Departamento de Obras Civiles, Universidad Técnica Federico Santa María, Valparaíso, Chile.

⁵ Research Center for Integrated Disaster Risk Management (CIGIDEN), ANID/FONDAP/15110017, Santiago, Chile.

⁶ Centro Científico Tecnológico de Valparaíso (CCTVal), ANID PIA/APOYO AFB180002, Valparaíso, Chile.

⁷ Richard Mowll Consulting Ltd, 154 Bing Lucas Drive, Tawa, Wellington 5028, New Zealand.

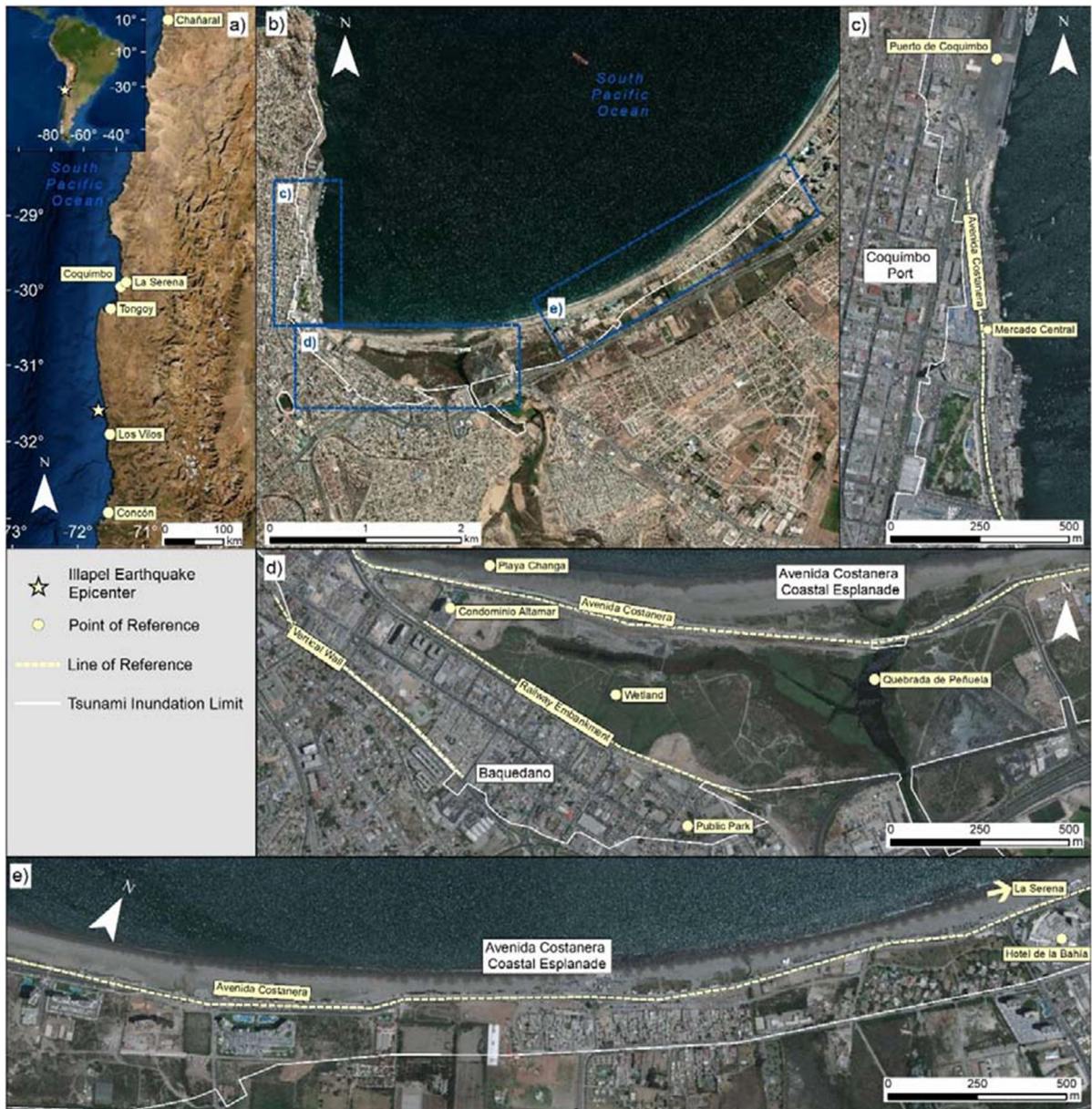


Figure 1

Locations of **a** the Illapel earthquake epicentre, **b** Coquimbo survey area and focused survey areas, **c** Coquimbo Port, **d** Baquedano neighbourhood and **e** Avenida Costanera coastal esplanade

building, infrastructure and environmental (i.e. wetland) damage observed in Coquimbo and Los Vilos (Fig. 1a). In Coquimbo (pop. 209,684), tsunami wave heights reached 4.75 m at the Port tide gauge, causing a maximum run-up height of 6.4 m (Aránguiz et al. 2016; Contreras-López et al. 2016). Aránguiz

et al. (2018) surveyed building damage in Coquimbo for 585 ‘mixed wood and masonry’ buildings in “destroyed” (118) and “not destroyed” (450) states. A fragility analysis determines 20% of tsunami exposed buildings reached or exceeded a destroyed damage state. The authors concluded that buildings

were mostly damaged by the tsunami impact as low earthquake shaking intensities were recorded at the Coquimbo area, e.g. 0.20–0.29 g (USGS, 2015).

Infrastructure network damage and disruption were cited in immediate tsunami damage reports (ONEMI 2015). Network component damage investigations were not a primary focus of national-led post-event surveys. Post-tsunami surveys prior to this event have mainly focused on systematic building damage assessments opposed to component damage sustained by transport, energy, water and telecommunications networks. Empirical information on tsunami hazard intensity, infrastructure component attributes and damage level are critical for analysing the fragility of individual network components. Infrastructure component fragility models can support investigations of potential service disruption to single or multiple networks affected by tsunamis.

This study presents 2015 Illapel Tsunami hazard characteristics, building and infrastructure network component damage observations and data from Coquimbo, Chile. We conducted a ‘census style’ field surveyed to record damaged and undamaged samples for a high proportion of tsunami exposed buildings, infrastructure components for transport, energy and water networks, and coastal protection structures. Here we report tsunami flow depths, building and infrastructure component damage levels and factors contributing to their damage. Finally, we discuss implications of ‘census style’ surveys for tsunami damage data collection and cascading impacts from co-located infrastructure component damage. The rich empirical dataset has been applied to investigate road component fragility in Coquimbo (Williams et al. 2020) and will inform future investigations of tsunami sources, inundation hazards and built-asset fragility investigations in Chile.

2. Field Survey

Field survey activities were conducted in Coquimbo from September 24th to 28th, eight days after the 2015 Illapel Tsunami. The survey aimed to measure and record the distribution of tsunami inundation traces (i.e. flow depth watermarks), and corresponding building and infrastructure network

component damage. Post-event reports indicated building and infrastructure component damage mostly occurred in the city of Coquimbo, though damage was also reported in Tongoy and Los Vilos. This focused the survey in built-up areas of Coquimbo, including Coquimbo Port, Baquedano neighbourhood (hereafter termed Baquedano), and the Avenida Costanera coastal esplanade toward La Serena (Fig. 1c–e). These areas are serviced by a range of infrastructure networks including transport, energy, water and coastal protection structures.

A digital survey was designed to record tsunami flow depths, along with building and infrastructure network component damage levels in Coquimbo. Data samples and observations were measured using the Real Time Asset Capture Tool (RiACT), an Android based application with configurable templating to enter and store spatial information on tsunami hazard characteristics and damage (Lin et al. 2019). Global positioning system (GPS) functionality enables accurate location positioning of tsunami traces and exposed building or infrastructure components.

Tsunami flow depths (Synolakis & Okal, 2005) were measured on damaged and non-damaged buildings and structures (e.g. fences, walls), and features (e.g. trees) in accordance with prescribed methods in UNESCO-IOC ITST (2014) guidelines. Recorded depths were measured as the ‘watermark’ indicating the maximum depth above ground. Watermarks indicating flow depths (e.g. ~ 0.1 m) were measured close to maximum run-up limits.

Damage levels and key physical and non-physical attributes of buildings and infrastructure components were recorded within the survey area (Fig. 1b). A ‘census style’ survey approach was applied where this information was for a high proportion of damaged and undamaged buildings, transport (roads, railways, pathways), energy (utility poles, fuel tanks), water (culverts, drain inlets, hydrants, manholes, pipelines, pump stations) and coastal protection structures (seawalls) exposed to tsunami inundation. Damage levels were categorised using an ordinal scale ranging from DL0 (No damage) to DL3 (Complete damage). The scheme’s four-level damage division is adapted from Peiris (2006) to support consistent damage level attribution for building and

infrastructure component types. Damage levels describe physical damage observed to building and components, indicating their potential for reinstatement to a pre-damaged condition (Table 1). Multiple damage level attribution is possible from on-ground surveys opposed to manual or automated remote sensing techniques that can limit attribution to dual damage levels e.g. ‘destroyed’ or ‘not destroyed’ (Koshimura et al. 2009; Mas et al. 2012). The damage scheme applied in Coquimbo supports consistent database development, compatible with field or remote sensed building and infrastructure component damage data from tsunami events in Chile or internationally.

Additional building and infrastructure component spatial information recorded included GPS coordinates, evidence of debris impact, scouring, debris or sediment deposition and physical and non-physical attributes. The construction frame, storeys and use (e.g. residential, commercial, industrial etc.) were recorded for each surveyed building, and primary and secondary attributes recorded for transport, energy and water network components, and coastal protection structures (Table 2). RiACT is limited to point data capture only which required the linear extents of road, railway, pathway, pipeline and seawall components to be recorded between two points indicating the start and end point of the damage samples. The linear extent between points were measured post-hoc using ArcGIS 10.4 software. Non-integer or decimal attribute values were pre-coded in RiACT with the option to record open answers or NA values, resulting in a nominal-, ordinal- and interval-scaled data structure.

3. *Tsunami Hazard*

Tsunami flow depths were measured at 655 locations within the survey area. (Fig. 2). Depths ranged from 0.1 to 4.7 m with a mean and standard deviation of 1.47 m and 1.02 m. A post-event time series analysis of sea surface elevation data recorded at the Coquimbo Port tide gauge, showed a maximum amplitude of 4.97 m above the reference level, with the second wave being the largest (Aránguiz et al. 2016). Implementation of the model by Cortés et al.

(2017) showed Coquimbo bay is prone to resonance, and the maximum amplitude of the first four resonant modes is reached in Coquimbo city. This is relevant here as many surveyed locations could have been exposed to more than one wave. Watermarks on some buildings and structures indicating flow depths from three potential tsunami waves were corroborated with anecdotal accounts from eyewitnesses. Where multiple watermarks were present, a single watermark was measured representing the maximum flow depth above ground level.

3.1. *Coquimbo Port*

In the Coquimbo Port (‘Puerto de Coquimbo’) area we measured maximum flow depths of 4.7 m from 97 watermarks on buildings and structures located on or near wharves. A mean depth of 2.39 m (1.24 m SD) was measured from 98 watermarks measured up to 172 m from the shoreline. Flow depths reduce in height from 3 to 4 m near the ‘Mercado Central’ in the south (cf. Figs. 1c, 2), to < 2 m near ‘Puerto de Coquimbo’ in the north. The inundation extent was limited north of Coquimbo Port due to steep topography and a narrow coastal plain.

3.2. *Baquedano*

The highest concentration of measured flow depths (359) was recorded from watermarks on buildings and structures in Baquedano. The mean flow depth of 1.54 m (0.9 SD) in Baquedano is nearly 1 m lower than depths measured in the Coquimbo Port, although depths at some sites exceeded 3 m. Inundation extents varied from 220 m near the southwest boundary to over 550 m toward the eastern boundary as the coastal plain widens. Notably, a vertical wall along the southwestern boundary of this survey area (Fig. 2) limited tsunami run-up. Flow depths up to 2.5 m measured on buildings within 100 m of the wall, are consistent with depths reported by Aránguiz et al. (2016). As the coastal plain toward the southeast widens, depths decrease eastward to 0.1 m to 0.15 m measured near the public park (Fig. 2). This area is afforded protection from a railway embankment located between the built-area

Table 1

Damage level descriptions for buildings and infrastructure network components in the Coquimbo survey area

Building or component	DL0 no damage	DL1 Partial damage, repairable	DL2 Partial damage, unreparable	DL3 Complete damage
Buildings	–	Damage to non-structural components only	Major damage to non-structural components and collapse of an external wall	Collapse of two or more external walls, columns or construction frame removed from foundations
Road	–	Minor damage to road surface, all lanes passable with caution	Major damage to one lane. One lane impassable	Major damage to whole carriageway, all lanes impassable
Bridge	–	Minor damage, often from impacts to the superstructure	Major damage to superstructure but still in place on piers, superstructure may have been shifted	Complete washout of superstructure
Pathway	–	Damage to path surface, minor damage to subgrade, passable with caution	Damage to path surface and subgrade, not passable	Complete damage to subgrade and surface, not passable
Railway	–	Minor scour of ballast, tracks in place	Scour to ballast, tracks pushed off ballast	Complete washout of ballast and tracks
Utility Pole	–	Scour or minor damage at base, pole in place	Buckling of pole, damage to pole base/foundation	Pole bent, snapped or sheared from base/foundations
Fuel Tank	–	Minor dents and surface scrapes, minor scour to foundations	Dents and scrapes to tank, footing bent, foundation scoured	Tanks sheared off footings, washed away
Culvert	–	Minor scour around culvert, may be blocked	Culvert heavily scoured out, but in place, scour or aggradation may render culvert useless	Culvert completely scoured out, washed away
Drain Inlet	–	Minor damage to grate, no damage to subsurface, temporary blockage or capacity reduction	Grate damaged, drain blocked, scour around drain, requires sediment removal or replacement	Drain inlet completely scoured out, washed away
Hydrant	–	Scour around base of hydrant, minor damage to hydrant, no leaks	Components sheared off, hydrant leaking	Hydrant sheared off base, pipe burst
Manhole	–	Minor scour around manhole/foundation, minor damage to cover	Moderate-major damage to manhole surface or cover, shaft in place	Manhole shaft scoured out, washed away
Pipeline	–	Minor scour to weak backfill, minor scrapes or dents to exposed pipes	Scour and exposure of buried pipes, scrapes and dents, minor-moderate leaks at joints	Exposed and washed away, free-flowing leaks at breaks and shears
Pump Station	–	Minor damage to components from low velocity water intrusion, infiltration of silt possible	Contamination and failure of electrical pumping equipment, sediment cover and debris impacts to structural components	Structural collapse, components sheared from footings and washed away, sediment cover
Seawall	–	Scour or aggradation around seawall, remains in place	Seawall rotated, tilted or separation from foundations and/or adjacent sections, some scour, to backfill	Seawall washed away, backfill scoured completely scoured

and wetland. Despite this protection, the furthest tsunami inundation observed occurred here, as inundation backfilled the built-up area landward of the embankment up to 700 m from the shoreline.

3.3. Avenida Costanera Coastal Esplanade

One hundred and ninety-nine watermarks recorded along the Avenida Costanera coastal

esplanade and built-areas near ‘Playa Changa’ beach show a gradual flow depth decrease eastward (Fig. 2). Depths ranged from 0.1 to 3.1 m, with a mean of 0.88 m (SD 0.68 m). At the western end of Avenida Costanera, flow depths up to 3 m were recorded at Condominio Altamar. Over a 4.7 km distance eastward of this location, depths decrease to 0.2 m to 0.5 m near Hotel de la Bahía. Flow depths were measured on both high and low-rise buildings, east of

Table 2

A summary of tsunami hazard and exposure information collected in Coquimbo from 24 to 28th September 2015

Hazard or exposure type	Primary attribute	Secondary attribute	Metric	Value
Tsunami	Flow depth	–	m	Decimal
Building		Construction Frame (Timber, Masonry, Reinforced Concrete, Steel)	–	Text
		Storeys	–	Integer
		Use (Commercial, Community, Education, Government, Industrial, Religious, Residential)	–	Text
Transport Network	Road	Use (Bridge, Pedestrian, Primary, Residential, Secondary, Service, Tertiary)	–	Text
		Surface Material (Asphalt, Concrete, Unsealed)	–	Text
		Lanes	–	Integer
		Length	m	Decimal
	Railway Pathway	Length	m	Decimal
Energy Network	Utility Pole	Component Type (Electricity, Street Light, Street Sign, Cellular Tower)	–	Text
		Construction Material (Concrete, Steel, Timber)	–	Text
		Height (< 5, > 5)	m	Text
	Fuel Tank	Use (Petroleum, LPG)	–	Text
Water Network		Component Type (Culvert, Drain Inlet, Hydrant, Manhole, Pipeline, Pump Station)	–	Text
		Diameter	mm	Decimal
		Network Type (Potable Water, Stormwater, Wastewater)	–	Text
Coastal Protection Structure	Seawall	Component Type (Curved-Steeped, Embankment, Irregular Face, Revetment, Rubble-mound, Vertical Wall)	–	Text
		Length	m	Decimal

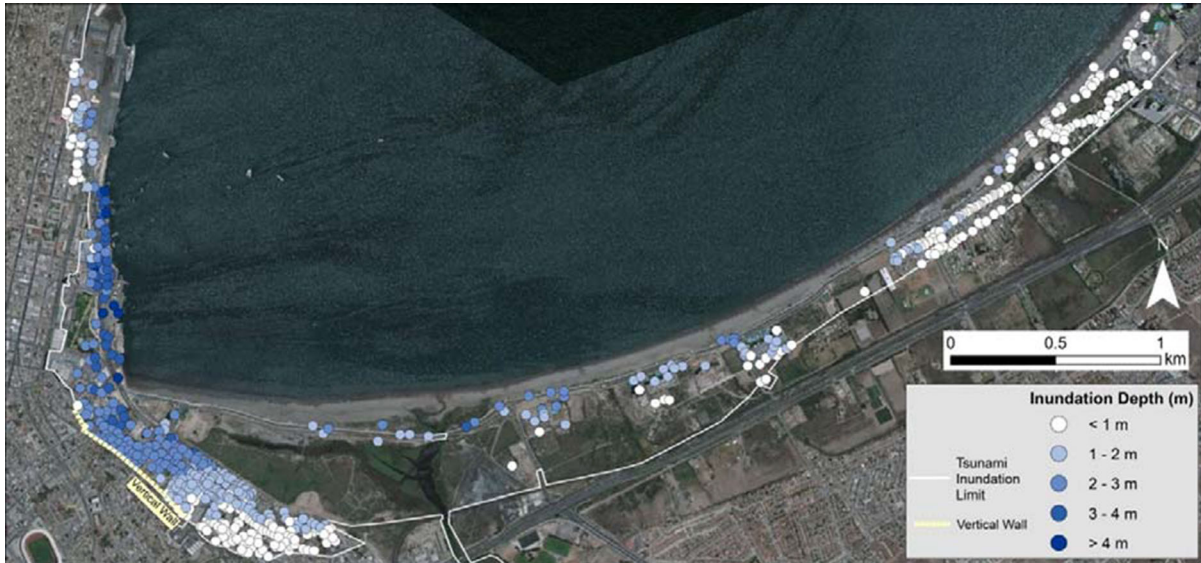


Figure 2
Tsunami flow depths measured in the Coquimbo survey area

the Quebrada de Peñuelas river. High-rise buildings within 1.5 km east of the river were exposed to depths up to 2.5 m. On low-rise buildings located

another 0.7 km east, maximum flow depths observed reduce to 1.2 m. In these built-areas, observed

inundation varied between 200 to 300 m from the shoreline.

4. Tsunami Impacts

4.1. Buildings

Over a four-day period, damage levels were recorded for 545 buildings (Fig. 3). Surveyed buildings were primarily used for residential, commercial (e.g. retail, restaurants) and industrial purposes. Construction frames are broadly classified as timber (106), ‘masonry’ (379), ‘reinforced concrete’ (14) and ‘steel’ (46). Flow depths measured at building locations ranged between 0.1 m and 4.5 m, with a mean of 1.01 m (SD 1.02 m).

The most common non-engineered construction frame building surveyed were ‘masonry’ (69%). Masonry buildings were most low-rise, comprising two stories or less (96%), comprising lightly reinforced concrete columns with concrete block infill walls often with timber frame additions for second stories or ‘lean-to’ structures attached to exterior walls (term ‘mixed structures’ by Aránguiz et al. 2018). Forty-three masonry buildings surveyed sustained complete damage in response to flow depths ranging from 1 to 3.8 m (mean 2.32 m; SD 0.86 m).

Most buildings (335) sustained partial damage, with 318 repairable (DL1) and 17 unrepairable (DL2). Unrepairable damage was observed due to external wall collapse or column failures (Fig. 4a), often occurring when depths exceeded 2 m. Most low-rise buildings (96%) sustained repairable damage when exposed to depths below 2 m, with damage observed when depths exceed 0.1 m to 0.2 m. Construction frames were undamaged in these cases (Fig. 4b) though, joinery, services and both internal and external doors and windows often required replacement. Only two tsunami exposed buildings surveyed sustained no damage (DL0) as the waves did not penetrate into the buildings.

‘Timber’ was a less frequent non-engineered construction frame surveyed (19%). Timber buildings were often informal structures that sustained complete damage when flow depths exceeded 2 m. A low proportion of buildings surveyed were engineered ‘reinforced concrete’ (2%) or ‘steel’ (8%) construction frames. These construction frames were common for high-rise multi-story condominiums and industrial or warehouse buildings. Although these buildings were exposed to measured flow depths up to 4.1 m (mean 1.86 m; SD 0.95 m), was limited to ground floor levels, damaging non-structural components. Reinforced concrete buildings sustained damage to external openings (i.e. doors and windows), internal

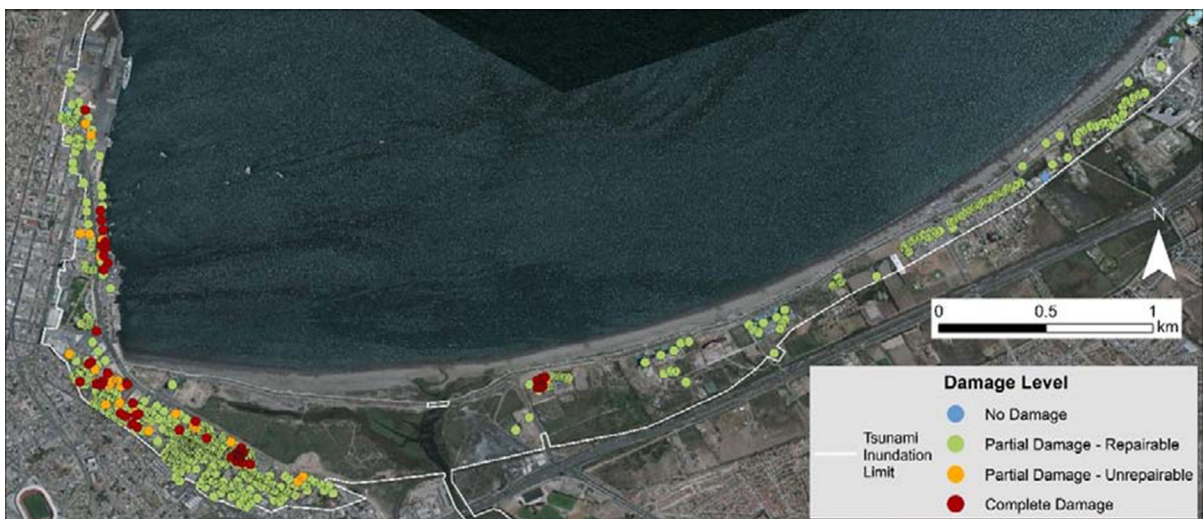


Figure 3
Surveyed building locations and damage levels

partitions and electricity and plumbing services. Steel buildings sustained removal of light sheet metal external wall cladding while steel columns often remained undamaged. Reinforced concrete and steel buildings surveyed were deemed to have sustained partial but repairable damage (DL1), with buildings being usable after repair.

4.2. Infrastructure Network Components

4.2.1 Transport

Roads Damage levels were recorded for over 25 km of roads (Fig. 5a). A high proportion (87%) of roads sustained no damage (DL0). Undamaged roads were commonly observed in Baquedano. Sheltering afforded by buildings, road and railway embankments and coastal protection structures in the survey area contributed to limiting most road damage (\geq DL1) within 250 m of the shoreline. Eye-witness accounts and drone footage indicated considerable disruption to undamaged roads particularly from debris deposition on local roads in the Baquedano and Coquimbo Port areas where vehicle transport was disrupted for several days after tsunami inundation. Debris and sediment deposition on roads were not recorded at the time of survey due to removal from post-tsunami clean-up activities.

Road damage (i.e. \geq DL1) ranging in length from 13 to 64 m, were recorded for residential and

Figure 5
Surveyed infrastructure component locations and damage levels surveyed for **a** transport, **b** energy, and **c** water networks, and **d** coastal protection structures

secondary roads near Coquimbo Port and Avenida Costanera tertiary road. Complete damage (DL3) for 1.1 km of roads was mostly observed along Avenida Costanera west of Quebrada de Peñuelas river. Here, we measured flow depths between 2 m to 3 m near sites where rubble-mound seawall and culvert failures instigated road embankment erosion and surface damage, making both lanes impassable (Fig. 6a). Avenida Costanera was also reduced to a single passable lane where these failures caused partial road damage (DL2). Complete and partial seawall and culvert damage observed on the seaward margin of Avenida Costanera indicates road damage was initiated by inland tsunami flows, opposed to return flows from water trapped in the wetland area (Fig. 1e). The Avenida Costanera coastal access road between Coquimbo and La Serena was completely disrupted for several days until temporary infill of scoured road embankment sections restored partial service for vehicles and pedestrians.

Pathways Pathways alongside roads provided pedestrian and cycling thoroughfares in the survey area. Over 30 km of pathways were inspected, constructed with concrete and brick paver surfaces.



Figure 4

Low-rise masonry buildings sustaining **a** partial but unreparable damage (DL2) from external wall collapse and column breakage and **b** partial but repairable damage (DL1) from first story inundation, indicated by flow depth watermarks present on the building exterior

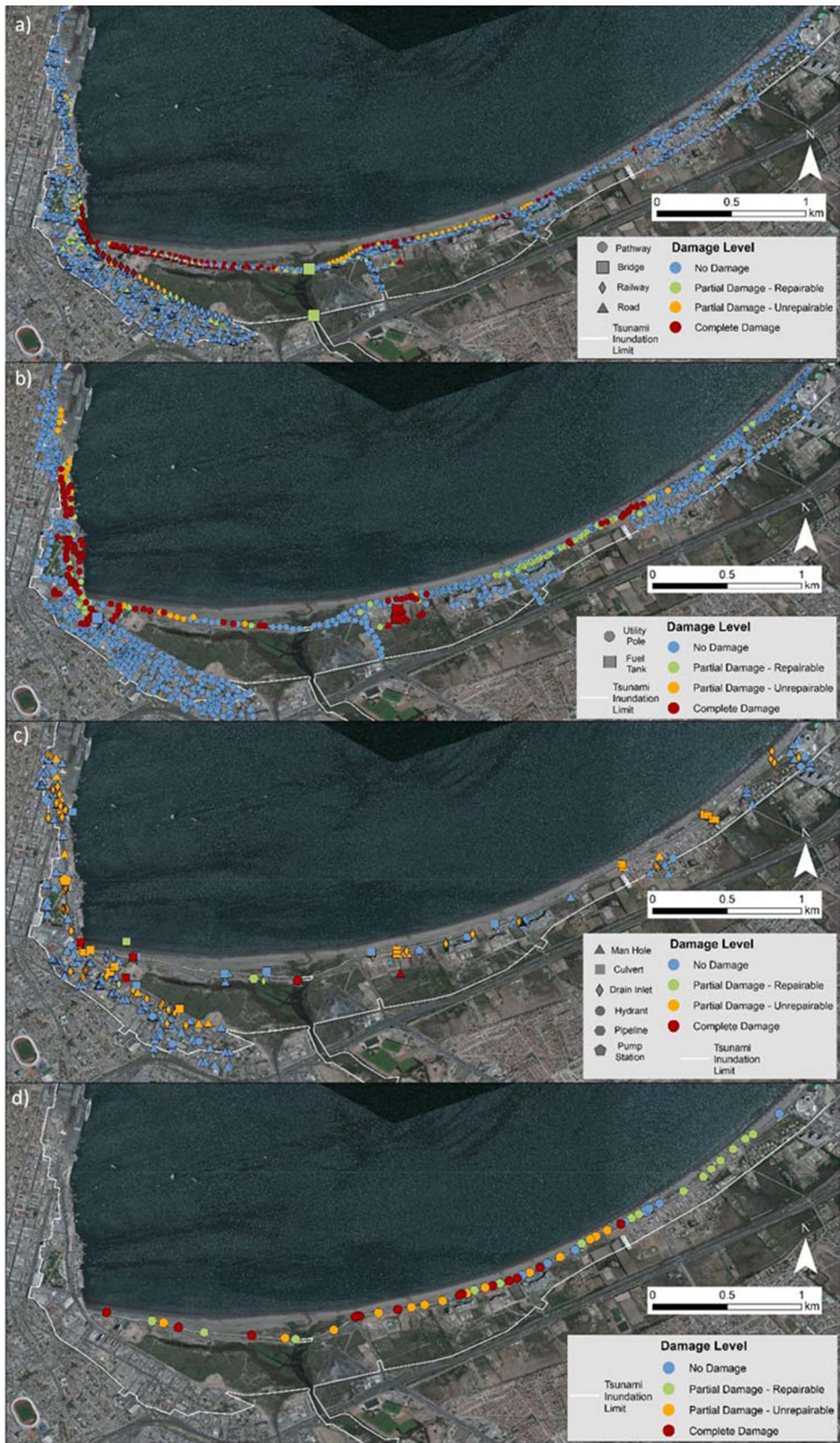




Figure 6

a Avenida Costanera road embankment and surface damage caused by culvert and seawall failure, **b** railway track warping and displacement, **c** utility pole failure from debris impact, **d** utility pole failure due to seawall failure and scouring, **e** pump station well exposed by superstructure removal, **f** seawall collapse causing pathway and road embankment damage on Avenida Costanera, with temporary fill to support transport service.

A high proportion (65%) of pathways were undamaged from inundation, particularly concrete surfaces located more than 100 m inland from the shoreline. Pathway damage was extensive along Avenida

Costanera (4.7 km), with complete damage (2.5 km) caused by road embankment erosion and surface damage in response to coastal protection structure or culvert failures. Tsunami wave overtopping of

seawalls caused the complete removal of brick pavers and scour of underlying embankment fill (DL3). Partial damage to pathways disrupted the Avenida Costanera thoroughfare for cyclists, though pedestrian use remained possible.

Railways A single 2.05 km railway track in the survey area connects Coquimbo Port to the national railway network. The railway track sustained 1.2 km of damage (\geq DL1), including 0.65 km of complete damage (DL3) in the Coquimbo Port area due to seawall failure. Here, reduced protection resulted in embankment scour, removing railway track support. Railway tracks embedded in road surfaces sustained no damage, while partial (DL1) to complete (DL3) damage was observed along a raised embankment immediately seaward of Baquedano. Embankment overtopping caused scour and loss of support for railway ties, resulting in track movement and deformation (Fig. 6b).

4.2.2 Energy

Utility Poles Local distribution networks transmitted electricity services using above ground cables attached to utility poles and below ground cables connecting street and traffic lights. The 1031 poles surveyed (Fig. 5b) often supported multiple above ground services including electricity and telecommunications cables, lights and signage. High proportions of poles supported electricity transmission (50%) or street-lights (45%), while poles dedicated to traffic signals (4%) and cellular transmission ($<$ 1%) were less frequently observed. Utility poles were mainly constructed of concrete (46%) and steel (50%) materials, with foundations either ground planted, or concrete foundation pad bolted.

Utility poles surveyed (80%) frequently experienced no damage (DL0) from tsunami inundation. Undamaged poles were observed for flow depths over 2 m though, electricity and telecommunication services were disrupted due damage to other poles carrying cables on the same distribution networks. Complete damage (DL3) was sustained by 10% of poles, often occurring in response to direct impact by debris, small boats and vehicles (47%) in the Coquimbo Port area (Fig. 6c). Where flow depths exceed 2.5 m utility poles may have also failed due to

debris loading on electricity service cables. Scouring of utility pole foundation support following seawall failure or road embankment erosion frequently caused their complete damage (40%) along the Avenida Costanera coastal esplanade (Fig. 6d). Scouring at the pole base initiated from wave overtopping of seawalls caused tilting or collapse, making poles unrepairable (DL2), while partial but repairable damage (DL1) was observed where bolts connecting base plates to foundation pads appeared to bend under pressure from hydrodynamic force without obvious signs of debris impact.

Fuel tanks Two steel tanks containing liquid petroleum gas (LPG) were inundated 115 m inland from Avenida Costanera (Fig. 5b). These tanks sustained complete damage from exposure to depths between 1.5 m to 2 m. This damage appeared to result from tank supports being sheared off from bolts attaching to their concrete slab foundation. These tanks were washed inland approximately 50–100 m from their original location but did not leak LP. In Baquedano, a petrol station exposed to depths reaching 2.5 m sustained no damage to concrete lined underground petroleum storage tanks. Despite these tanks being undamaged, petrol pump damage disrupted petroleum services for an estimated two weeks.

4.2.3 Water

Nodes Water infrastructure components were surveyed for 314 stormwater (culverts, drain inlets, manholes) and potable water (hydrant, pump station) infrastructure network nodes (Fig. 5c). Several culverts embedded in the Avenida Costanera road embankment were washed away (DL3), removing both lanes thereby disrupting vehicle and pedestrian transport services. Culvert failures could have occurred from contraction scour as described by Duc and Rodi (2008), whereby inundation contracted through the structure, increases flow velocity and shear stress at the culvert outlet causing scour. Return flows from the first wave may have initiated this process at seaward outlets with successive waves scouring road subgrade surrounding culverts causing loss of lateral support removing some culverts entirely from the road embankment. Partial damage

(DL2) requiring replacement was observed culvert fracturing or breakage when undermined by scour at seaward outlets. Drain inlets and manholes inset in road surfaces and sidings frequently sustained low damage levels (\leq DL1) however, manhole cover removal and deposition of sediment and debris required post-event clean-up for the continuation of stormwater services.

A potable water pump station 350 m south of Coquimbo Port was exposed to flow depths up to 3 m. Complete damage was sustained by both the masonry building superstructure (Fig. 6e), as well as plant and equipment (e.g. pumps, electrical circuitry, pipes). In-ground filters were partially damaged and reusable following clean-up and repair, while sediment and debris deposited in the dry well required removal. Hydrants, providing access to water main pipes sustained no or partial damage (DL1) when exposed to flow depths up to 2 m.

Pipelines A gravity fed steel water main pipe servicing the Coquimbo urban area was severed where it crossed a reinforced concrete bridge on Avenida Costanera. Although the bridge superstructure only sustained partial damage (DL1) from flow depths 2 to 3 m above ground, erosion of the unprotected abutment caused an adjacent manhole to fail, breaking the pipe (DL3). Scour and removal of underlying unconsolidated materials also caused the pipe to suspend, requiring sand piles to temporarily weigh down the pipe at the time of survey.

4.2.4 Coastal Protection Structures

Seawalls A continuous rubble-mound seawall on the Playa Changa beach armoured the Avenida Costanera road embankment from Coquimbo Port to Quebrada de Peñuelas river. East of the river a vertical wall afforded protection to the road and pathways. Damage levels were recorded for 1.65 km of rubble-mound seawalls and 3.83 km vertical seawalls. Damage (\geq DL1) was observed for over 4.8 km of seawalls, including the entire rubble-mound seawall length (Fig. 5d). Partial damage (DL1) occurred over 1.57 km, where rocks were displaced at wave overtopping locations. Partial, but irreparable damage (DL2) was observed over 1.76 km, where wave overtopping scoured rubble-mound or vertical wall

backfill causing rotational failures and partial seawall collapse. Complete rubble-mound seawall damage (DL3) from rock removal or displacement, and back fill and subgrade scour and erosion exceeded 1 km. Scour of unconsolidated materials on the seaward edge vertical seawalls led to undermining and partial or complete collapse. Seawall failures exacerbated scouring of Avenida Costanera road embankment, damaging the road surface and pathways (Fig. 6f). Complete damage up to 600 m in length were observed for rubble-mound seawalls west of the Quebrada de Peñuelas river, while vertical wall damage lengths did not extend beyond 80 m east of the river. The smaller seawall damage lengths observed coincide with relatively lower flow depths (< 2 m) measured on adjacent buildings and structures compared to Coquimbo Port and Baquedano.

5. Discussion

Post-event field surveys are critical for detailing the hazard characteristics and built-asset impacts of tsunami events. The 2015 Illapel Earthquake generated tsunami was the subject of several hazard and damage surveys conducted by national and international survey teams (Aranguiz et al. 2016; Tomita et al. 2016; Contreras-López et al. 2016). The moderate size tsunami (i.e. flow depths ~ 4 m; horizontal inundation ~ 700 m) and limited geographical exposure of buildings and infrastructure components provided ideal conditions to collect a high-resolution flow depth and damage dataset. Our survey activities employed a ‘census style’ approach, whereby information for a high proportion of inundated buildings and infrastructure in damaged and non-damaged states is recorded by a digital survey. This enabled a small field team of five researchers to record 655 flow depths, 546 building and 2544 infrastructure component damage samples in four days. The survey ~ 7.5 km² area benefited the ‘census style’ approach however, for major tsunami events the geographic extent of inundation and damage, or access restrictions to severely damaged sites could limit its application. For future major tsunami events, such as those produced by great subduction earthquakes, ‘census style’ surveys could

focus small damage areas (e.g. $< 10 \text{ km}^2$), specific building or infrastructure component typologies or co-located infrastructure component locations.

The 'census style' survey in Coquimbo recorded tsunami flow depths and physical and non-physical attribute information for both damaged and undamaged buildings and infrastructure network components. Survey timing eight-days after the tsunami, meant clean-up and recovery activities had removed debris and damaged structures or services (e.g. electricity cables) impeding vehicle and pedestrian movements in the survey area. These activities limited the ability to observe service disruption and outage times for components such as roads. Despite clean-up and recovery activity progress we noticed high proportions of undamaged (i.e. DL0) components exposed to inundation. This included 825 utility poles and 22 km and 26 km of roads and pathways respectively. These components sustained minimal damage from flow depths up to 2 m unless impacted by secondary hazards such as tsunami entrained debris or scouring and erosion. Undamaged samples are usually absent in empirical datasets collected from tsunami events (Eguchi et al. 2013). The inclusion of undamaged building and infrastructure components in fragility analysis determines the tsunami hazard intensities where damage is both unlikely, and likely to occur. This supports development of credible cumulative distribution functions determining a building or components probability of reaching or exceeding a physical damage level or state as tsunami hazard intensity increases (Tarbotton et al. 2015).

Infrastructure network components in Coquimbo were often subject to secondary hazards or cascading impacts where components are co-located. Utility poles carrying electricity services were relatively resistant to complete damage when exposed to flow depths less than 2 m. However, we observed complete damage to 5% of utility poles in response to tsunami entrained vehicles or boats impacting poles or electrical cables, particularly in the Coquimbo Port area. Utility poles also sustained complete damage in response to scour and foundation support loss following seawall and culvert failures or wave overtopping along Avenida Costanera. Here, complete damage of roads and pathways further resulted

from seawall and culvert failures. Complete damage of co-located roads, pathways and utility poles at some locations caused both transport and energy network service outage for the Avenida Costanera coastal esplanade. Electricity and transport networks continued servicing Coquimbo Port and Baquedano shortly after the tsunami, though cascading impacts across multiple co-located network components highlights a requirement for infrastructure operators to mitigate potential service disruption caused from other network component damage. Infrastructure component fragility analysis in response to increasing tsunami hazard intensities will enable spatial assessments of single and cascading network component damage and service disruption (Dong et al. 2020; Kilanitis & Sextos, 2019).

The empirical building and infrastructure network component damage data from Coquimbo extends built-asset damage datasets from previous Chilean (Koshimura et al. 2011; Mas et al. 2012) and global (MLIT, 2012; Murao & Nakazato, 2010; Reese et al. 2011; Suppasri et al. 2011, 2012) tsunami events. Digital information on tsunami hazard characteristics at building and infrastructure component locations is critical for understanding their fragility to physical damage (Tarbotton et al. 2015). A limitation of the survey data collected was the ability to directly attribute flow depths or other tsunami hazard characteristics to infrastructure components. Damage data application in future component fragility or network impact analysis then requires spatial sampling of an event-based hydrodynamic inundation model output (i.e. map) or interpolated water surface to determine hazard characteristics such as flow depth (m), flow velocity (m/s) and hydrodynamic force (kN/m) at surveyed component sites. Multiple component damage observed in Coquimbo from seawall and stormwater culvert failures indicates flow velocity and force are important hazard characteristics determining the fragility of single infrastructure components and potential cascading impacts across multiple infrastructure networks.

6. Conclusions

In this study, we present an empirical building and infrastructure network component damage dataset for the 2015 Illapel Tsunami in Coquimbo, Chile. The dataset was derived from a digital ‘census style’ field survey conducted eight days after the tsunami to measure and record inundation characteristics and associated damage to buildings and transport, energy, water infrastructure network components and coastal protection structures. This survey approach was possible due to the relatively modest spatial extent ($\sim 7.5 \text{ km}^2$) of tsunami inundation and damage observed in Coquimbo.

Over a four-day period, 655 flow depths and 3000 damage samples for tsunami exposed buildings and infrastructure components were recorded by a small field team of five researchers. Damage levels for 545 buildings showed most sustained partial but repairable damage (DL1). A further 2544 damage samples were collected for transport, energy, water infrastructure network components and coastal protection structures. These samples provided extensive coverage of transport (25 km roads; 2 km; railway; 30 km pathways) and electricity (1031 utility poles) network components. A high proportion of components sustained ‘no damage’ despite exposure to depths exceeding 2 m. Low earthquake shaking intensity in the Coquimbo area implied infrastructure components were undamaged at the time of tsunami inundation.

We observe that complete damage to infrastructure components was often caused by secondary hazards (e.g. debris) or cascading impacts. Utility poles carrying electricity services were resistant to complete damage at flow depths less than 2 m, but often failed due to contact with tsunami entrained debris such as small boats and vehicles. Seawall and stormwater culvert failures also cause complete damage to co-located roads, pathways and utility poles. Investigation of the hydrodynamic tsunami characteristics determining infrastructure component fragility will support future assessments of damage to single components and cascading impacts across multiple infrastructure networks.

Acknowledgements

The authors are sincerely grateful to the people of Coquimbo for supporting our field survey activities. Authors thank the Chilean Navy Hydrographic and Oceanographic Service (SHOA), National Emergency Office (ONEMI) and Universidad de Valparaíso for hosting the field survey team for onsite visits and supporting survey activities through logistics and damage information provision. The authors also acknowledge all supporters of the survey including: Auckland Council, Earthquake Commission (EQC), GNS Science (Project: RiskScape), Ministry of Foreign Affairs and Trade (NZ); National Institute of Water and Atmospheric Research (Project: CARW1603; CARH2106); New Zealand Society of Earthquake Engineering; University of Canterbury (Ministry of Business, Innovation and Employment’s Natural Hazard Research Platform contract C05X0907). PAC also thanks ANID through its grants Research Center for Integrated Disaster Risk Management (CIGIDEN), ANID/FONDAP/15110017 and PIA/APOYO AFB180002. PAC has been partially funded by Research Center for Integrated Disaster Risk Management (CIGIDEN), ANID/FONDAP/15110017 and by Centro Científico Tecnológico de Valparaíso, (CCTVal), ANID PIA/APOYO AFB180002.

Publisher’s Note Springer Nature remains neutral with regard to jurisdictional claims in published maps and institutional affiliations.

REFERENCES

- Aránguiz, R., González, G., González, J., et al. (2016). The 16 September 2015 Chile tsunami from the post-tsunami survey and numerical modeling perspectives. *Pure and Applied Geophysics*. <https://doi.org/10.1007/s00024-015-1225-4>
- Aránguiz, R., Urrea, L., Okuwaki, R., et al. (2018). Development and application of a tsunami fragility curve of the 2015 tsunami in Coquimbo, Chile. *Natural Hazards and Earth System Sciences*. <https://doi.org/10.5194/nhess-18-2143-2018>
- Contreras-López, M., Winckler, P., Sepúlveda, I., et al. (2016). Field survey of the 2015 Chile tsunami with emphasis on coastal wetland and conservation areas. *Pure and Applied Geophysics*. <https://doi.org/10.1007/s00024-015-1235-2>

- Cortés, P., Catalán, P. A., Aránguiz, R., et al. (2017). Tsunami and shelf resonance on the northern Chile coast. *Journal of Geophysical Research*. <https://doi.org/10.1002/2017JC012922>
- Dong, S., Yu, T., Farahmand, H., et al. (2020). Bayesian modeling of flood control networks for failure cascade characterization and vulnerability assessment. *Computer-Aided Civil and Infrastructure Engineering*. <https://doi.org/10.1111/mice.12527>
- Duc, B. M., & Rodi, W. (2008). Numerical simulation of contraction scour in an open laboratory channel. *Journal of Hydraulic Engineering*. [https://doi.org/10.1061/ASCE0733-9429\(2008\)134:4\(367\)](https://doi.org/10.1061/ASCE0733-9429(2008)134:4(367))
- Eguchi, R. T., Eguchi, M. T., Bouabid, J., et al. (2013). *HAZUS Tsunami Benchmarking*. (pp. 1–48). Validation and Calibration.
- Fritz, H. M., Petroff, C. M., Catalán, P. A., et al. (2011). Field Survey of the 27 February 2010 Chile Tsunami. *Pure and Applied Geophysics*. <https://doi.org/10.1007/s00024-011-0283-5>
- Kilanitis, I., & Sextos, A. (2019). Integrated seismic risk and resilience assessment of roadway networks in earthquake prone areas. *Bulletin of Earthquake Engineering*. <https://doi.org/10.1007/s10518-018-0457-y>
- Koshimura, S., Matsuoka, M., Matsuyama, M., et al. (2011). Field Survey of the 2010 Tsunami in Chile, in: 8th Int. Conf. on Urban Earthquake Engineering, April 2010, 1–13.
- Koshimura, S., Oie, T., Yanagisawa, H. et al. (2009). Developing fragility functions for tsunami damage estimation using numerical model and post-tsunami data from Banda Aceh, Indonesia. *Coastal Engineering Journal*. <https://doi.org/10.1142/S0578563409002004>
- Lin, S. L., King, A., Horspool, N., et al. (2019). Field data collection framework development and applications. *Frontiers in Built Environment*. <https://doi.org/10.3389/fbuil.2019.00015>
- Mas, E., Koshimura, S., Suppasri, A., et al. (2012). Developing tsunami fragility curves using remote sensing and survey data of the 2010 Chilean Tsunami in Dichato. *Natural Hazards and Earth System Sciences*. <https://doi.org/10.5194/nhess-12-2689-2012>
- MLIT (Ministry of Land, Infrastructure and Transportation). Archive of the Great East Japan Earthquake Tsunami disaster urban reconstruction assistance survey (2012), available at: <http://fukkou.csis.u-tokyo.ac.jp/>. Accessed 4 July 2020.
- Murao, O., & Nakazato, H. (2010). Vulnerability functions for buildings based on damage survey data in Sri Lanka after the 2004 Indian Ocean tsunami. In: Proceedings of the 7th International Conference on Sustainable Built Environment (ICSBE-2010) Kandy, Kenya 371–378.
- ONEMI. Monitoreo por Sismo de Mayor Intensidad (2015), available at: <https://www.onemi.gov.cl/alerta/se-declara-alerta-roja-por-sismo-de-mayor-intensidad-y-alarma-de-tsunami/>. Accessed 6 July 2020.
- Peiris, N. (2006). Vulnerability Functions for Tsunami Loss Estimation in: First European Conference on Earthquake Engineering and Seismology, Geneva, Switzerland, Paper No. 1121.
- Reese, S., Bradley, B., Bind, J., et al. (2011). Empirical building fragilities from observed damage in the 2009 South Pacific tsunami. *Earth Science Reviews*. <https://doi.org/10.1016/j.earscirev.2011.01.009>
- Suppasri, A., Koshimura, S., & Imamura, F. (2011). Developing tsunami fragility curves based on the satellite remote sensing and the numerical modeling of the 2004 Indian Ocean tsunami in Thailand. *Natural Hazards and Earth System Sciences*. <https://doi.org/10.5194/nhess-11-173-2011>
- Suppasri, A., Mas, E., Koshimura, S., et al. (2012). Developing tsunami fragility curves from the surveyed data of the 2011 Great East Japan tsunami in Sendai and Ishinomaki plains. *Coastal Engineering Journal*. <https://doi.org/10.1142/S0578563412500088>
- Synolakis C., Okal E. (2005). 1992–2002: Perspective on a Decade of Post-Tsunami Surveys. In: Satake K. (eds) *Tsunamis. Advances in Natural and Technological Hazards Research*, vol 23. Springer, Dordrecht. https://doi.org/10.1007/1-4020-3331-1_1
- Tarbotton, C., Dall’Osso, F., Dominey-Howes, D., et al. (2015). The use of empirical vulnerability functions to assess the response of buildings to tsunami impact: comparative review and summary of best practice. *Earth Science Reviews*. <https://doi.org/10.1016/j.earscirev.2015.01.002>
- Tomita, T., Arikawa, T., Takagawa, T., et al. (2016). Results of post-field survey on the Mw 8.3 Illapel earthquake tsunami in 2015. *Coastal Engineering Journal*. <https://doi.org/10.1142/S0578563416500030>
- UNESCO (2014). International Tsunami Survey Team (ITST) Post-Tsunami Survey Field Guide. 2nd Edition. IOC Manuals and Guides No.37, Paris: UNESCO 2014 (English).
- USGS (2015). M 8.3 – 48 km W of Illapel, Chile (2015), available at: <https://earthquake.usgs.gov/earthquakes/eventpage/us20003k7a/technical>. Accessed 6 July 2020.
- Williams, J. H., Wilson, T. M., Horspool, N., et al. (2020). Assessing transportation vulnerability to tsunamis: utilising post-event field data from the 2011 Tōhoku tsunami, Japan, and the 2015 Illapel tsunami, Chile. *Natural Hazards and Earth System Sciences*. <https://doi.org/10.5194/nhess-20-451-2020>
- Ye L., Lay T., Kanamori H., Koper K.D. (2017). Rapidly Estimated Seismic Source Parameters for the 16 September 2015 Illapel, Chile Mw 8.3 Earthquake. In: Braitenberg C., Rabinovich A. (eds) *The Chile-2015 (Illapel) Earthquake and Tsunami*. Pageoph Topical Volumes. Birkhäuser, Cham. https://doi.org/10.1007/978-3-319-57822-4_2